

Parametric and numerical modeling tools to forecast hydrogeological impacts of a tunnel

Metodi parametrici e modellazione numerica per la previsione degli impatti idrogeologici di una galleria

Valentina Vincenzi^a , Leonardo Piccinini^b, Alessandro Gargini^c, Michele Sapigni^d

^aStudio Geologico Vincenzi Valentina, Via Nives Gessi 3, 44122, Ferrara - Italy -  email: info@idrogeologiavincenzi.it

^bDipartimento di Geoscienze, Università degli Studi di Padova, Padova - Italy - email: leonardo.piccinini@unipd.it

^cDip. Scienze Biologiche, Geologiche e Ambientali, Alma Mater Studiorum-Università di Bologna, Bologna-Italy-email: alessandro.gargini@unibo.it

^dEnel GreenPower S.p.A, Via Torino 16, 10132 Venezia-Mestre - Italy - email: sapigni.michele@enel.com

ARTICLE INFO

Ricevuto/Received: 7 October 2010
Accettato/Accepted: 18 November 2010
Ripubblicato online/Republished online:
30 March 2022

Publication Note - This paper has been published previously (DOI: 10.4409/Am-021-10-0017), in the international journal "AQUAmundi". AQUAmundi closed in 2015 and published papers officially disappeared, being available only in secondary, personal or organizations' repositories. However, the contents of this paper are still considered of interest for readers, who suggested that Acque Sotteranee - *Italian Journal of Groundwater* reprint it, so here it is republished in its original form, with minor updates limited to references and data, provided in footnotes.

Citation:

Vincenzi V, Piccinini L, Gargini A, Sapigni M (2022) Parametric and numerical modeling tools to forecast hydrogeological impacts of a tunnel. *Acque Sotteranee - Italian Journal of Groundwater*, 11(1), 51 - 69
<https://doi.org/10.7343/as-2022-558>

Correspondence to:

Valentina Vincenzi 
info@idrogeologiavincenzi.it

Keywords: tunnel, groundwater inflow, forecasting, spring, impact.

Parole chiave: galleria, venute di acque sotterranee, previsione, sorgente, impatto.

Copyright: © 2022 by the authors. License Associazione Acque Sotteranee. This is an open access article under the CC BY-NC-ND license: <http://creativecommons.org/licenses/by-nc-nd/4.0/>

Abstract

The project of interest involving a hydroelectrical diversion tunnel through a crystalline rock massif in the Alps required a detailed hydrogeological study to forecast the magnitude of water inflows within the tunnel and possible effects on groundwater flow. The tunnel exhibits a length of 9.5 km and is located on the right side of the Toce River in Crevoladossola (Verbania Province, Piedmont region, northern Italy). Under the geological framework of the Alps, the tunnel is located within the Lower Penninic Nappes in the footwall of the Simplon Normal Fault, and the geological succession is mostly represented by Antigorio gneiss (meta-granites) and Baceno metasediments (metacarbonates). Due to the presence of important mineralized springs for commercial mineral water purposes, the abovementioned hydrogeological study focused on both quantity and quality aspects via rainfall data analysis, monitoring of major spring flow rates, monitoring of hydraulic heads and pumping rates of existing wells/boreholes, hydrochemical and isotopic analysis of springs and boreholes and hydraulic tests (Lefranc and Lugeon). The resulting conceptual model indicated dominant low-permeability (aquitard) behavior of the gneissic rock masses, except under conditions of intense fracturing due to tectonization, and aquifer behavior of the metasedimentary rocks, particularly when interested by dissolution. Groundwater flow systems are mainly controlled by gravity. The springs located near the Toce River were characterized by high mineralization and isotopic ratios, indicating long groundwater flow paths. Based on all the data collected and analyzed, two parametric methods were applied: 1) the Dematteis method, slightly adapted to the case study and the available data, which allows assessment of both potential inflows within the tunnel and potential impacts on springs (codified as the drawdown hazard index; DHI); 2) the Cesano method, which only allows assessment of potential inflows within the tunnel, thereby discriminating between major and minor inflows. Contemporarily, a groundwater flow model was implemented with the equivalent porous medium (EPM) approach in MODFLOW-2000. This model was calibrated under steady-state conditions against the available data (groundwater levels inside wells/piezometers and elevation and flow rate of springs). The Dematteis method was demonstrated to be more reliable and suitable for the site than was the Cesano method. This method was validated considering a tunnel through gneissic rock masses, and this approach considered intrinsic parameters of rock masses more notably than morphological and geomorphological factors were considered. The Cesano method relatively overestimated tunnel inflows, considering variations in the topography and overburden above the tunnel. Sensitivity analysis revealed a low sensitivity of these parametric methods to parameter values, except for the rock quality designation (RQD) employed to represent the fracturing degree. The numerical model was calibrated under ante-operam conditions, and sensitivity analysis evaluated the influence of uncertainties in the hydraulic conductivity (K) values of the different hydrogeological units. The hydraulic head distribution after tunnel excavation was forecasted considering three scenarios, namely, a draining tunnel, tunnel as a water loss source, and tunnel sealed along its aquifer sectors, considering 3 levels of K reduction. Tunnel impermeabilization was very effective, thus lowering the drainage rate and impact on springs. The model quantitatively defined tunnel inflows and the effects on spring flow at the surface in terms of flow rate decrease. The Dematteis method and numerical model were combined to obtain a final risk of impact on the springs. This study likely overestimated the risk because all the values assigned to the parameters were chosen in a conservative way, and the steady-state numerical simulations were also very conservative (the transient state in this hydrogeological setting supposedly lasts 1–3 years). Monitoring of the tunnel and springs during tunnel boring could facilitate the feedback process.

Riassunto

Il progetto di costruzione di una galleria di derivazione attraverso rocce cristalline nelle Alpi occidentali ha richiesto un dettagliato studio idrogeologico finalizzato alla previsione delle venute d'acqua in galleria e dei possibili effetti sulla circolazione idrica sotterranea. Il tunnel ha una lunghezza di 9,5 km e si trova lungo il fianco destro del Fiume Toce nei pressi di Crevoladossola (Provincia di Verbania, Regione Piemonte). Dal punto di vista geologico regionale, il tracciato della galleria attraversa le Falde Pennidiche Inferiori costituite da potenti falde gneissiche (meta-graniti; Verampio, Antigorio, M. Leone) alternate a più sottili orizzonti metasedimentari (principalmente meta-carbonati; Teggiolo e Baceno) in origine corrispondenti all'originaria copertura triassico-cretacica del basamento cristallino. Questa struttura a sandwich ha assunto l'attuale conformazione a duomo durante il sollevamento a letto della faglia normale del Sempione. La presenza, nei pressi del tracciato, di importanti sorgenti mineralizzate utilizzate a scopo potabile e commerciale ha imposto uno studio idrogeologico basato sia su dati quantitativi che qualitativi (misure di precipitazione, monitoraggio delle portate delle sorgenti, monitoraggio dei livelli piezometrici nei sondaggi e risultati di prove di emungimento in pozzi e sondaggi esistenti, prove idrauliche Lefranc e Lugeon nei sondaggi e monitoraggi idrochimici e isotopici sulle sorgenti e sui sondaggi). Dall'analisi del modello geologico e dei dati idrochimici è stato definito il modello idrogeologico concettuale di riferimento che assegna un comportamento acquitardo alle rocce gneissiche, ad eccezione delle fasce tettonizzate e fratturate, ed un comportamento acquifero ai metacarbonati in particolare dove interessati da fenomeni di dissoluzione. Le sorgenti localizzate sul fondovalle del fiume Toce, caratterizzate da una maggiore mineralizzazione e maggiori rapporti isotopici, costituiscono il recapito di lunghi percorsi sotterranei all'interno di un sistema di flusso idrico sotterraneo essenzialmente controllato dalla gravità. Sulla base del modello geologico e di tutti i dati raccolti sono state effettuate previsioni d'impatto con due metodi parametrici e un modello numerico. Il primo metodo parametrico utilizzato, leggermente modificato per adattarlo al caso in esame, ha consentito di valutare sia le potenziali venute d'acqua in galleria sia i possibili impatti sulle sorgenti (definiti come Drawdown Hazard Index; DHI); il secondo metodo parametrico ha consentito solamente la determinazione delle potenziali venute d'acqua in galleria discriminando tra maggiori e minori. Parallelamente è stato costruito un modello numerico alle differenze finite (MODFLOW-2000) dell'intero massiccio montuoso assumendo un comportamento poroso equivalente (EPM) e calibrato in condizioni stazionarie sulla base dei livelli piezometrici nei pozzi e sondaggi e sulla base della quota e portata delle sorgenti. Il metodo Dematteis si è dimostrato più affidabile e adeguato al caso specifico rispetto al metodo Cesano; infatti, il primo, validato su una galleria in rocce gneissiche, assegna maggiore importanza ai parametri intrinseci degli ammassi rocciosi piuttosto che ai fattori morfologici e geomorfologici. Il metodo Cesano sovrastima, relativamente agli altri metodi, le potenziali venute d'acqua in galleria assegnando più importanza alle variazioni topografiche ed allo spessore della copertura rocciosa della galleria. È stata effettuata un'analisi di sensitività sia per i metodi parametrici che per il modello numerico; i primi hanno evidenziato variabilità legata essenzialmente al valore di RQD (Rock Quality Designation, utilizzato come rappresentativo delle condizioni di fratturazione), il modello numerico è risultato influenzato dall'incertezza sui valori della conducibilità idraulica degli ammassi rocciosi. Gli effetti dello scavo sulla superficie piezometrica, preventivamente simulate in condizioni ante-operam, sono stati simulati utilizzando, nel modello numerico, tre possibili condizioni: galleria drenante, galleria disperdente ed infine galleria impermeabilizzata in corrispondenza dei settori acquiferi (con assegnazione di crescenti livelli di riduzione della permeabilità). Il trattamento dei settori acquiferi è risultato particolarmente efficace riducendo il drenaggio e gli impatti sulle sorgenti; il modello è in grado di definire quantitativamente le venute d'acqua in galleria e gli effetti sulle sorgenti in termini di riduzione della portata. L'assegnazione del livello di rischio finale per ciascuna sorgente è stato definito incrociando i risultati del modello numerico con quelli del metodo Dematteis; tali livelli di rischio sono, tuttavia, da considerarsi sovrastimati in quanto i valori assegnati a ciascun parametro sono stati scelti conservativamente ed altrettanto conservativamente si possono considerare le condizioni stazionarie generate dal modello numerico dato che, in questo tipo di ammassi rocciosi, è probabile che le condizioni transitorie si protraggano da 1 a 3 anni. Il monitoraggio delle venute d'acqua in galleria durante il futuro scavo e il proseguimento dei monitoraggi sulle sorgenti consentirà una verifica dei modelli e fornirà importanti informazioni sperimentali.

Introduction

In mountain regions, tunnel excavation can threaten groundwater to the highest degree, but this threat has not been considered of great importance in the past, as demonstrated by various Italian case studies, such as the very high groundwater level drawdown and spring dewatering as a consequence of Gran Sasso highway tunnel boring activities (Petitta and Tallini 2002), but also in recent times, such as the impact on streams and springs of the tunnels of the Bologna-Florence high-speed railway line (Gargini et al. 2006, 2008). As a consequence, in recent years, the public and authorities have become increasingly sensitive to these problems, and scientific attention has been drawn to the possibility of forecasting the effects of tunnels and underground excavations on groundwater inflows and water table drawdown and evaluating the risk to springs located in hydrogeological basins crossed by underground openings.

Forecasting the impacts of a given draining tunnel on groundwater flow systems is one of the most challenging tasks in engineering geology. Tunnel drainage can produce severe effects on hydrogeological systems, either under transient or steady-state conditions, such as spring drying, hydraulic head drawdown, well yield shortages, and stream base flow depletion. The resulting environmental, sociosanitary and economic damage, if forecasted at the early project stage, should be addressed with risk mitigation measures (alternative tunnel pathways, tunnel sealing, and even project abandonment) within the framework of a technically correct cost-benefit analysis.

In hard rock aquifers, it is extremely difficult to forecast either major inflow occurrences along a tunnel or associated effects on surface water and groundwater due to the highly heterogeneous distribution of the hydraulic conductivity (K) and consequent notable dependence of major inflows on interception by localized geological features (i.e., fractured zones, faults, and karst conduits). The geometry and location of these structures can be determined through a suitable 3D geological model (geological mapping, aerial image interpretation and geophysical surveys) with an approximate range of tens or hundreds of meters, and in a few cases, relevant hydraulic parameters can be assessed via permeability tests performed in deep boreholes.

Two evaluation tools have been considered to overcome these uncertainties and obtain good forecasts: parametric methods and mathematical models. Parametric methods, also referred to as matrix methods, identify relevant physical quantities (such as the RQD, permeability, overburden, and faults intersecting the tunnel), and these variables and their interactions are ranked by assigning ratings and multipliers to obtain final probability indexes of the impacts on springs. Parametric methods for impact assessment evaluation can be matrix-based or rating- and weight-based methods. In the first case, a contingency matrix is developed, thereby combining relevant parameters: the classical example is the Leopold matrix for environmental impact assessment (EIA) purposes (Leopold 1971). In the second case, a parameterization system

of ratings and multiplier weights is applied to variables considered relevant to obtain final quantification indices: typical examples are given by the DRASTIC (Aller et al., 1985) and SINTACS R5 (Civita and De Maio 2000) methods, which are employed for aquifer intrinsic vulnerability assessment.

In contrast, mathematical groundwater flow modeling simulates the actual process causing the impact with a physically based approach. Adopted simulation codes vary from simple analytical equations, assuming Darcyan groundwater flow, simple and stationary boundary conditions and a homogenous or simple K distribution (Zhang and Franklin 1963; Goodman 1965; Barton 1974; Federico 1984; Lei 1999, 2000; El Tani 1999), to complex numerical codes, which are more flexible and adjustable to real-world conditions but much more exigent in terms of scientific expertise, financial resources and input data.

In the case study presented here, the occurrence of important mineralized springs developed for commercial mineral water necessitated robust risk analysis. The potential impacts on springs of a draining tunnel were evaluated via two methods: parametric probabilistic and numerical deterministic methods. Both methods started from a detailed hydrogeological study necessary to establish a conceptual model, and the final drawdown risk for each spring was obtained by combining these two methods. This paper presents the main results, together with the effectiveness of these two approaches in performing the above risk analysis.

Geological setting

The diversion tunnel layout crosses the deepest part of the Penninic units traditionally assigned to the ancient northern margin overthrust by oceanic and southern austroalpine margins during the continental collision period of alpine orogenesis. Present-day deep topographic erosion allows a glimpse into the structure of the Lepontine nappes, tectonic units formed by flat recumbent folds comprising orthogneissic cores with discontinuous micaschistic and paragneissic outer zones overlying Mesozoic metasediments (Schmidt and Preiswerk 1905; Castiglioni 1958; Milnes et al. 1981; Steck 2008) (Fig. 1). The latter consist of calcschists, dolomitic and calcitic marbles, quartzites and discontinuous gypsum and anhydritic horizons. This petrographic and rheologic sandwich pattern is the result of many deformative phases, the most important of which sliced and thrust the former continental, mainly granitic, crust onto the sedimentary cover with displacements of tens of kilometers (Maxelon and Mancktelow 2005). The amphibolitic metamorphic conditions achieved in the main deformation phase allowed mineralogical transformations yielding pervasive axial plane foliation forming the present-day schistosity and most prominent weakness planes of the rock mass. Successive slightly or nonmetamorphic folding events provided the nappe pile with its present dominant structure visible along the Antigorio valley (Fig. 2) with a flat-laying attitude in its central part, around the so-called Verampio window, transitioning into a steep southward inclination near Crevoladossola (Mancktelow

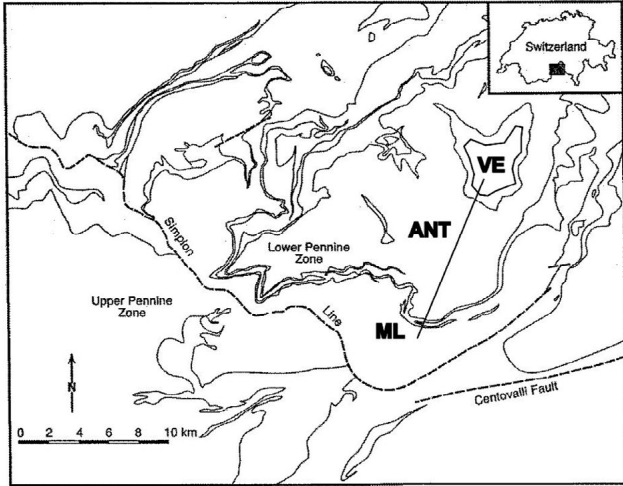


Fig. 1 - Geological sketch of the area between the Verampio window (VE) and Simplon Fault (modified from Grasemann and Mancktelow, 1993). ANT: Antigorio gneiss; ML: Monte Leone gneiss. The line represents the trace of the cross section depicted in Figs. 2 and 3.

Fig. 1 - Schema geologico dell'area compresa tra la finestra di Verampio (VE) e la Faglia del Sempione (modificato da Grasemann & Mancktelow, 1993). ANT: gneiss di Antigorio; ML: gneiss di Monte Leone. La linea rappresenta la traccia della sezione trasversale di Fig. 2 e Fig. 3.

1985; Grasemann and Mancktelow 1993). The N-S cross section (Fig. 3) shows the geologic and hydrogeologic structures of the mountain ridge and corresponds to the trace of the diversion tunnel, as shown in the geological map of Figure 2. The main feature is represented by the thick late Variscan (ca. 340 My) Antigorio unit, composed of a monotonous leucocratic orthogneiss only rarely exhibiting any structural or petrographic diversity (Bigioggero et al. 1977). To the north, this unit overlays the deepest alpine unit corresponding to late Variscan Verampio granitic gneiss and host rock represented by garnet-rich Baceno micaschists. Interlayered between these two large tectonic units occurs the most important permeable unit (Baceno metasediments), whose stratigraphy has been suitably defined upon drilling of three deep boreholes. This unit exhibits an average thickness of approximately 70 m and consists of a lower gypsum-anhydrite layer and at least two cohesionless sugary carbonate horizons, namely, dolomitic marbles and calcschists. To the south, the geological structure is characterized by a late nonmetamorphic kilometer-scale fold linked to exhumation of the nappe pile along the extensional Simplon Fault (Campani et al. 2010). Near the southern portal, the tunnel trace crosses the second metasedimentary unit (Teggiolo) approximately

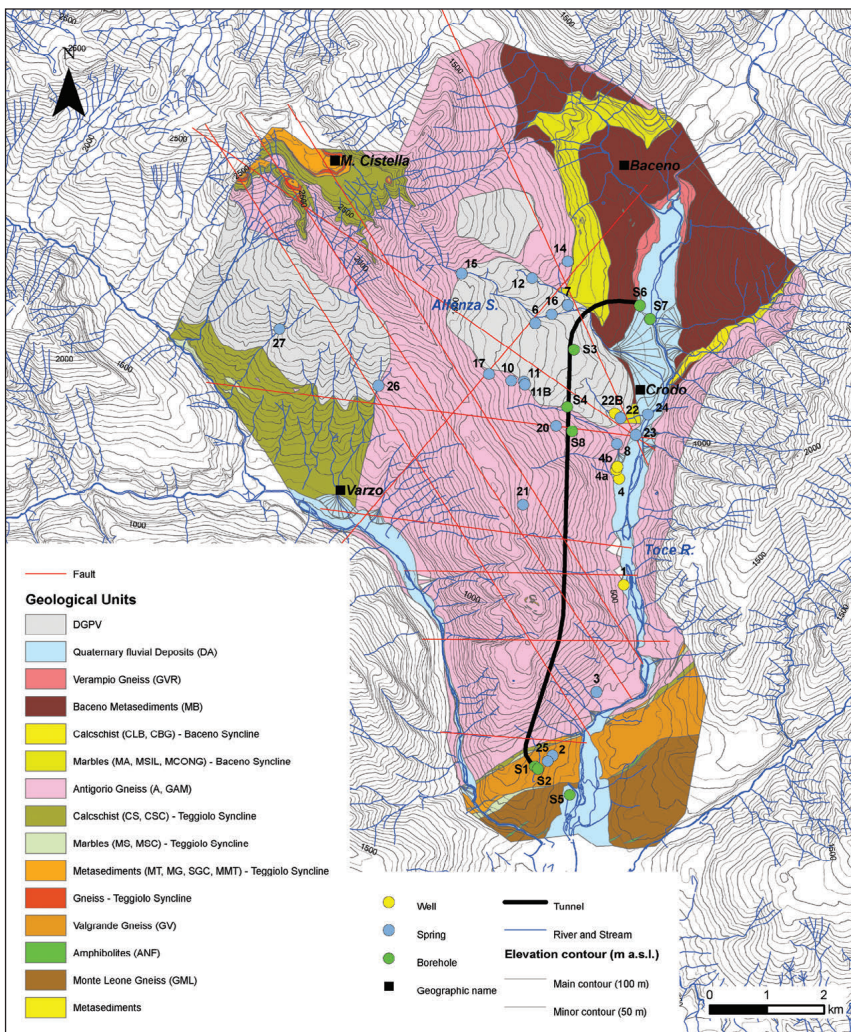


Fig. 2 - Geological map of the study area, with the groundwater monitoring points.

Fig. 2 - Carta geologica dell'area di studio, con ubicazione dei punti di monitoraggio delle acque sotterranee.

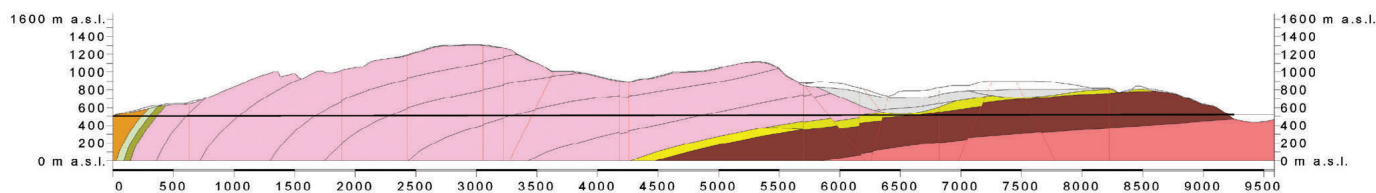


Fig. 3 - Geological section along the tunnel; the colors adhere to the geological legend of Fig. 2.

Fig. 3 - Sezione geologica longitudinale allo sviluppo della galleria; legenda geologica in Fig. 2.

70 m thick with a composition very similar to that of the Baceno metasediments. The tunnel trace ends in the third gneissic continental unit (Valgrande gneiss) mainly including fine-grained quartz-micaschists and gray biotitic gneiss.

Detailed geological mapping, borehole analysis and geophysical characterization allowed both reconstruction of a reliable 3D model and recognition of a large deep-seated landslide (deep-seated gravitational deformation, DSGD) in the northern part of the section possibly genetically linked to the underlying weak metasedimentary horizon. The whole triangular ridge is cross-cut by many brittle faults arranged in two main sets oriented along the NW-SE and E-W directions. These faults are the product of the last brittle exhumation phase of the Lepontine dome along the Simplon Fault (Bistacchi and Massironi 2000; Grosjean et al. 2004; Zwingmann and Mancktelow 2004).

Materials and methods

Hydrogeological characterization

The occurrence of important mineralized springs reserved for commercial mineral water exploitation requires a hydrogeological study focused on both the quantity and quality of groundwater, which was developed by applying different tools.

Rainfall data analysis, based on 8 meteorological stations, was performed to estimate the recharge rate to the aquifers. The water surplus in the modeled area was calculated via the Thornthwaite and Mather (1957) soil water balance method.

A census of the main water points was available, in addition to one year of hydrogeological monitoring data under ante-operam conditions encompassing 21 major springs and 5 wells in the area (Tab. 1a,b). Furthermore, 8 boreholes drilled for the project were available for hydrogeological monitoring (Tab. 1a). The available data (collected by the CESI S.p.A.) included the flow rates of the springs and groundwater levels of the wells and boreholes, measured monthly. The discharge variability index (DVI) was calculated for all springs as $(Q_{max}-Q_{min})/Q_{av}$, where Q_{max} is the maximum flow rate, Q_{min} is the minimum flow rate and Q_{av} is the average flow rate relative to the monitored year. The α coefficient (recession coefficient according to Maillet 1905) for each spring was derived from recession curves in the available data.

Combined with flow and piezometric measurements, in situ physico-chemical parameters were measured with

a multiparameter probe (temperature, specific electrical conductivity, pH, dissolved oxygen and dissolved carbon dioxide).

In the laboratory, ionic concentrations of fluoride, chloride, sulfate, nitrate, sodium, potassium, magnesium and calcium and the alkalinity, dissolved silica and fixed residue were measured in groundwater samples collected monthly. The concentrations of iron (total), strontium and lithium were measured twice a year at 5 monitoring points (11, 12, 22b, 23 and 24; Table 1a). The isotopic ratios of δ^2H , $\delta^{18}O$ (standard VSMOW, similar to Craig 1961) and $\delta^{13}C$ (standard PDB, similar to Urey et al. 1951) were measured monthly at the 4 most important monitoring points (11, 22, 23 and 24, chosen for their high discharge rates and drinking and commercial use).

The main data concerning water point monitoring and classification (springs, boreholes and wells), originating from both the census and data interpretation, are summarized in Table 1a, b.

Geological units were classified with respect to the permeability type (porous or fractured media) and expected K value, which was derived from the combined application of geological and geomorphological information available in the literature. Permeability tests (Lefranc and Lugeon tests) were performed in the 8 boreholes in the area, and other tests were performed 30 years ago in the planning phase of the Piedilago-Agaro plant, located 7 km to the north but transecting the same geological units (Martinotti per ENEL Produzione 1993).

The springs were classified according to Civita (1973, 2005), and joint analysis of all the data allowed us to establish the required hydrogeological conceptual model.

Parametric methods

A parametric method applied to tunnel impact forecasting basically involves a risk assessment where the risk of damage occurring to groundwater as a result of tunnel drainage is evaluated. The general equation (Einstein, 1988) to analyze tunnel impacts is:

$$R=H*P*Va*V \quad (1)$$

where R is the risk, e.g., the occurrence probability of a certain impact on groundwater flow systems; H is the hazard, e.g., the magnitude of the impact process, e.g., a

Tab. 1a - Main hydrogeological and hydrochemical data of the springs.

Tab. 1a - Principali dati idrogeologici e idrochimici delle sorgenti.

ID	Name	Type	Altitude (m a.s.l.)	Average flow rate (L/s)	IVP	α (d ⁻¹)	Hydrochemical facies
2	Bisogno	Spring	890	0.02			
3	Oira	Spring	420	11.17	0.83	1.29E-02	Ca-HCO ₃ -SO ₄
6	Viceno	Spring	850	3.07	0.31	6.50E-04	Ca-Mg-SO ₄ -HCO ₃
7	La Valle	Spring	850	5.38	0.28	3.00E-04	Ca-HCO ₃
8	Vegno	Spring	510	1.55	2.19	2.33E-02	Ca-Mg-SO ₄ -HCO ₃
10	Flecchio alta	Spring	1170	0.23	1.22	1.11E-02	Ca-HCO ₃
11	Flecchio	Spring	1100	14.22	0.73	1.13E-02	Ca-HCO ₃
11b	Flecchio Isolata	Spring	1090	3.23	1.47		Ca-HCO ₃
12	Longio	Spring	1140	16.04	0.49		Ca-HCO ₃
14	Trona	Spring	1050	1.37	0.88	3.10E-03	Ca-HCO ₃
15	Alfenza Nord	Spring	1420	12.46	1.05		Ca-HCO ₃
16	Alfenza sud	Spring	874	2.31	0.91	2.95E-03	Ca-HCO ₃
17	Cavoraga-Faiò	Spring	1300	0.08	1.38	9.40E-03	Ca-HCO ₃ -SO ₄
20	Ronconi	Spring	890	0.56	0.96	1.19E-02	Ca-HCO ₃
21	Cheggio	Spring	1390	0.06	1.19	1.91E-02	Ca-HCO ₃ -SO ₄
22	Cesa Inferiore	Spring	545	0.20	0.74	2.10E-03	Ca-HCO ₃
23	Valle Oro	Spring	457	19.97	0.11	6.60E-03	Ca-SO ₄
24	Lisiel	Spring	470	34.96	0.06	4.00E-04	Ca-SO ₄ -HCO ₃
25	La Conca	Spring	470	0.18	1.00	4.55E-03	Ca-HCO ₃
26	La Rocca	Spring	1100	15.00			
27	Calantagine	Spring	1420	35.00			

Tab. 1b - Main hydrogeological and hydrochemical data of the wells and boreholes.

Tab. 1b - Principali dati idrogeologici e idrochimici di pozzi e sondaggi.

ID	Name	Type	Altitude (m a.s.l.)	Depth (m)
1	Sarizzo	Well	386	30
4	Molinetto1	Well	424	101
4a	Molinetto2	Well	424	54
4b	Molinetto3	Well	424	71
22b	Cesa	Well	573	33
S1		Borehole	508	11.3
S2		Borehole	529	35.5
S3		Borehole	883	376
S4		Borehole	792	304
S5		Borehole	308	30
S6		Borehole	518	15
S7		Borehole	517	15
S8		Borehole	811	412

major inflow at the tunnel face; P is the hazard probability that a major inflow could occur along the tunnel; Va is the receptor value, which reflects the environmental, hydrologic and socio/economic importance of springs, streams and wells (surface emergence of groundwater flow systems) potentially subject to impact; and V is the vulnerability, intended as the expected damage related to major inflow occurrence due to hydrogeological connection between the tunnel and receptors.

Two methods, validated against case histories in metamorphic rocks similar to those in our study, were chosen: the DHI or Dematteis method (Dematteis et al. 2001) and the Cesano method (Cesano et al. 2000). These methods consider multiple sets of parameters, thus increasing the confidence in probabilistic evaluation with respect to the single-parameter method (Thapa et al. 2005). These methods were partially modified for the intended application to overcome either the lack of data measured at the tunnel drilling face (the study was conducted in ante-operam conditions), required for the application of the original methods, or specific intrinsic limitations of the method in the final DHI output.

The whole tunnel trace (approximately 9,000 m) was divided into 50.1-m sectors, with a total of 183 sectors (progressively numbered from the northern to the southern portal). The average elevation of each sector was assigned at the center, depending on the linear gradient (9.05‰) between the two main portal elevations, from 513.3 m (north) to 505 m a.s.l. (south).

21 springs and 5 wells were considered potential impact receptors for DHI evaluation, according to the hydrogeological conceptual model. The hydrogeological structure, groundwater flow circuit depth and spring hydrochemistry contributed to defining the degree of hydrogeological connection between the receptors and tunnel sectors.

Application of the DHI method

The DHI method is a typical rating- and weight-based parametric method to evaluate the risk which ranks the probability of spring flow depletion related to the inflow probability occurrence and spring vulnerability. The risk is expressed via an index denoted as the drawdown hazard index (DHI). It involves a fully coupled model (Jiao and Hudson 1995) and considers the physical relationships among different variables.

The method was applied through two steps: first, variables affecting the probability of potential inflow (PI) generation within tunnel sectors were rated and weighted; second, the obtained PI value was further weighted depending on the local vulnerability to obtain the final DHI value.

The original equations, retrieved from Dematteis et al. (2001), are:

$$PI(n) = (0.41 * FF(n) + 0.22 * RMP(n) + 0.20 * PZ(n) + 0.17 * OV(n)) \quad (2)$$

$$DHI(\text{spring}) = (PI)(\text{average}) * (IF+1) * (ST+1) * (DT+1) \quad (3)$$

where FF is the rock mass fracture frequency, RMP is the rock mass hydraulic conductivity, PZ is the thickness of the plastic zone around the bored tunnel, OV is the tunnel overburden, including Quaternary deposits, IF is the occurrence of hydrogeologic connection between the spring and tunnel, ST is the spring type, related to the depth of the groundwater flow system, and DT is the geometric distance between the tunnel sector and spring.

The DHI values are categorized into four piezometric drawdown risk classes with a relative probabilistic output, as indicated in Table 2.

With respect to the original formulation (please refer to Dematteis et al. 2001) the following changes were introduced.

FF variable: the rock quality designation (RQD) index (Deere et al. 1969; Deere and Deere 1989), derived from boreholes S1-S2-S3-S4 and S8, was considered representative of the FF variable because geomechanical surveys at the drilling face were not available. An arithmetic mean RQD value was calculated for each geological unit. The obtained results were integrated with data acquired from geomechanical

surveys performed on rock mass outcrops (Astolfi and Sapigni 1999). As a further refinement, the fracture occurrence at the megascale was derived from photoaerial lineament traces intersecting the tunnel trace, and this parameter was considered as follows: if a lineament occurred within a 250-m cylindrical buffer zone coaxial with the tunnel, the FF rating for the involved tunnel sectors along a ± 100 m linear distance from the lineament was reduced by one or two rating classes if one or more than one lineament, respectively, was involved.

K: permeability values were assigned to the different rock masses considering both the Lugeon test results and reference data, available in the literature, corresponding to metamorphites within an analogous geological framework (Loew 2002). Moreover, the K values were increased by 1 order of magnitude for tunnel sectors crossed by a fault or main fracture (with a ± 50 m buffer zone) determined with a longitudinal geologic profile and for sectors crossing the contact between the Antigorio gneiss and Teggiolo syncline due to their important and recognized aquifer behavior.

OV: this was determined from the tunnel longitudinal section, measured at the midpoint of the corresponding sector, and the value varied between 28 and 801 m.

PZ: according to a conservative approach, the PZ value was always considered three times the maximum calculated excavation disturbed zone (EDZ), reaching a conservative value of 14.7 m.

IF: 100-m or 50-m buffer zones were defined on each side of the primary or secondary structural lineaments (obtained through field geological surveys or aerial photo interpretation), respectively. If a spring was located in the buffer zone and, at the same time, the lineament crossed the tunnel, the spring IF value was set to 1 (otherwise, the value was set to 0). Springs discharging from Quaternary deposits were always assigned a 0 rating because these deposits were never involved in tunnel boring.

ST: three main groundwater flow systems were identified according to spring classification, namely, shallow, deep and mixed, which were assigned rating values of 0, 1 and 0.5, respectively.

DT: the Euclidean distance (i.e., the minimum geometrical distance) between the midpoint of each tunnel sector and the receptors was calculated independently of the relative elevation of the receptor with respect to the tunnel. The DT value ranged from 8907 to 244 m.

Application of the Cesano method

The Cesano method is not a codified parametric method but generates multiregression analysis results between potential tunnel inflows and influencing variables within an analogous hydrogeological framework (gneissic fractured aquifer below a Quaternary overburden with a variable thickness) representing an 80-km long tunnel in southern Sweden (Cesano et al. 2000). This method was chosen as a supplementary evaluation tool, thereby proposing a different set of PI factors to better verify the results. The Cesano method does not evaluate DHI but only PI, discriminating

Tab. 2 - DHI classes according to the Dematteis method.

Tab. 2 - Classi di DHI secondo il metodo Dematteis.

DHI	DHI classes
< 0.2	Absence of (or minimal) Drawdown
0.2 ÷ 0.6	Moderate Drawdown
0.6 ÷ 0.7	From moderate to severe Drawdown
> 0.7	Spring drying-up

major inflows from diffuse seepage. Four major inflow factors, among many others, were recognized and are listed here in order of importance: TSW = tunnel proximity to the main surface water body (i.e., streams, lakes, or reservoirs); BM = bedrock morphology underlying the Quaternary cover; T = topography; BFF = bedrock aquifer fracture density. Four diffuse seepage factors, among many others, were recognized and are listed here in order of importance: BM = bedrock morphology underlying the Quaternary cover; QC = thickness and lithology of the Quaternary cover; QA = area of the Quaternary outcrops above the tunnel; PV = BM peak and valley occurrences.

The main change introduced into the Cesano method was the transformation of multifactor correlation analysis in the original method into a rating- and weighting-based parametric method by summing the correlation coefficients and normalizing the result to 1. In this manner, weighted linear combinations of rates allowed coherent comparison to the Dematteis method. The weights derived for the Cesano method are presented in Table 3.

The relevant variables were parameterized as follows:

TSW was expressed based on the Euclidean distance between the midpoint of each tunnel sector and the nearest main stream bed located above the tunnel. The TSW values varied between 9930 and 22 m. The whole range was divided into 5 classes with an equal amplitude.

BM and T: these two variables were derived via comparison of a digital elevation model to the tunnel longitudinal geological section, considering 200-m tunnel sectors to better represent the top of the bedrock and topographic surface elevation changes. The maximum rating (1) was applied to bedrock troughs (areas of potential concentrated recharge), while the minimum rating (0) was assigned to mounds. A rating of 0.5 was assigned as an intermediate BM value. The T values ranged from 505 to 1299 m a.s.l.

BFF: both primary and secondary megascale tectonic lineaments were considered to obtain the FF Dematteis variable. The total number of lineaments crossing the tunnel (divided into 100-m long tunnel sectors) was calculated as follows: ratings of 1, 0.7, 0.35 or 0 were assigned to the tunnel sector if the number of lineaments was ≥ 3 , 2, 1, or 0, respectively.

QC was derived from the tunnel longitudinal geological section. The maximum thickness value reached 260 m, corresponding to the DSGD mass. The whole QC range was rated according to 5 classes of an equal amplitude.

QA: the outcropping areal extension (m^2) of QC within a 100-m long cylindrical search volume coaxial with the tunnel with a 1000-m radius was calculated, as derived from the geomorphological map and DEM. The values ranged from a maximum of 9800 m^2 (the tunnel sector was completely covered by Quaternary deposits; a maximum rating of 1) to a minimum of 0 m^2 (0 rating).

PV: peaks and valleys in the bedrock occurrence were identified from the tunnel longitudinal geological section, according to discrete 100-m long tunnel sectors. Ratings of 0

and 1 were assigned to peaks and valleys, respectively, and a rating of 0.5 was assigned to all the other sectors.

Tab. 3 - a) Weights for the major inflow factors; b) weights for the diffuse seepage factors (Cesano method).

Tab. 3 - a) Pesì corrispondenti ai fattori delle venute d'acqua principali; b) Pesì corrispondenti ai fattori di drenaggio diffuso (metodo Cesano).

a) Major inflow factor	Weight	b) Diffuse dripping factor	Weight
TSW	0.32	BM	0.30
BM	0.29	QC	0.29
T	0.28	QA	0.26
BFF	0.11	PV	0.11

Numerical model

Analytical codes, which are generally useful within limited tunnel sector and time-scale frames (Loew, 2002), were excluded because these codes are too simplistic given the complex hydrogeologic setting. A three-dimensional groundwater flow model was developed based on MODFLOW-2000 code (McDonald and Harbaugh 1988; Harbaugh et al. 2000), which solves the flow equation for saturated media according to the finite difference method.

Assuming that along the 9.2-km diversion tunnel, the groundwater flow system at the whole mountain ridge scale follows Darcy's law, the equivalent porous medium (EPM) approach was employed. This approach jointly considers the rock matrix and fractures and assigns these components bulk hydrodynamic properties across a rock volume sufficiently wide to be considered statistically representative (i.e., the representative elementary volume or REV; Long et al. 1982; Kanit et al. 2003). Within the REV, it could be assumed that the fracture distribution is consistent and uniform and that the fracture width does not allow turbulent flow. The geometric and hydrodynamic properties of distinct fractures are not required, small computational efforts are necessary, and good results can be obtained considering wide modeling areas (Mun and Uchrin 2004).

A rectangular model domain of 12000 m x 17000 m was set up, oriented parallel to the Gauss Boaga coordinate system and extending from Torrente Diveria in the north to Crevoladossola in the south (Fig. 2). On the horizontal plane, the domain was subdivided into cells of 100 m x 100 m, except for the zone including the tunnel and main springs where grid refinement yielded 25 m x 25 m cells (Fig. 4). Great effort was invested to obtain an effective vertical discretization result, and 20 variable-thickness layers were adopted. Layer 11 was employed to represent the tunnel plane and exhibited a thickness that included the plastic zone. The domain vertically extended from the topographic surface, as derived from the DEM, to an almost horizontal plane with an elevation of 510 m a.s.l., with a very gentle gradient parallel to the tunnel slope. The total thickness of the model varied between 350 and 3000 m. A section of the domain parallel to the tunnel trace is shown in Figure 5.

The hydraulic conductivity (K) was always regarded as an isotropic property, except for the normal faults/fracture zones, where an anisotropy factor of 10 was necessary along the x and z axes in the calibration process. The final K values, obtained after calibration, assigned to the 15-K zones are summarized in Table 4: every geological unit was represented by two K values, of which the first value represented the normally fractured rock mass, and the second value represented the rock mass affected by a fault/lineament. The K zone distribution is shown in Figures 4 and 5.

Recharge of the aquifer was simulated based on the 2nd type of boundary condition (b.c.) applied to each cell of the 1st saturated layer. The low sensitivity of the model to recharge allowed us to apply a uniform value of 270 mm/yr. The regional gradient was represented by the 1st type of b.c. on the northern side of the domain, with the maximum head value below the mountain ridge (1800 m a.s.l.), which decreased to 1045 m a.s.l. eastward and to 1250 m a.s.l. westward. The rivers bordering the model on the western and eastern sides representing discharge points of the regional groundwater

Tab. 4 - Hydraulic conductivity assigned to the different K zones (in m/s).

Tab. 4 - Conducibilità idraulica assegnata alle diverse zone di K (m/s).

Zone	Color	Hydrogeological Unit	Kx	Ky	Kz
1		Antigorio gneiss	1.00E-07	1.00E-07	1.00E-07
2		Quaternary fluvial deposits	5.00E-05	5.00E-05	5.00E-05
3		DGPV	7.00E-07	7.00E-07	1.00E-07
4		Metasediments (Baceno syncline)	5.00E-06	5.00E-06	5.00E-06
5		Baceno micaschists	1.00E-07	1.00E-07	1.00E-07
6		Verampio gneiss	1.00E-08	1.00E-08	1.00E-08
7		Metasediments (Teggiolo syncline)	5.00E-06	5.00E-06	5.00E-06
8		Valgrande gneiss	1.00E-07	1.00E-07	1.00E-07
9		Monte Leone gneiss	1.00E-07	1.00E-07	1.00E-07
10		Fault in Antigorio gneiss	7.00E-06	7.00E-06	7.00E-06
11		Fault in Metasediments (Baceno syncline)	1.00E-05	1.00E-05	1.00E-05
12		Fault in Baceno micaschists	5.00E-07	5.00E-07	5.00E-07
13		Fault in DGPV	1.00E-06	1.00E-06	1.00E-06
14		Quaternary glacial deposits	5.00E-06	5.00E-06	1.00E-06
15		Slope debris	5.00E-04	5.00E-04	5.00E-04

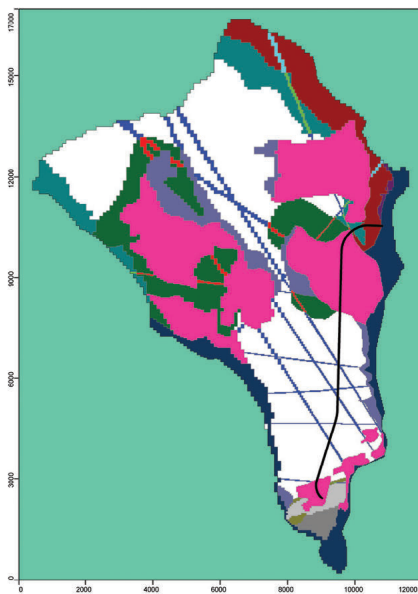


Fig. 4 - Flow domain and K zones in layer 1 of the MODFLOW model. The colors correspond to the K zones according to Table 3; inactive cells are marked with green; the coordinate axis is expressed in m; the tunnel trace is indicated in black.

Fig. 4 - Dominio di flusso e zone di K sul layer 1 del modello MODFLOW. I colori corrispondono a quelli di Tab. 3; le celle inattive sono rappresentate con il colore verde acqua; assi in metri; traccia della galleria in nero.

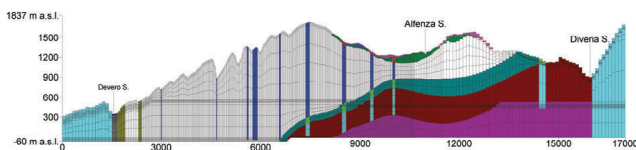


Fig. 5 - Section of the model domain along the tunnel trace (N-S direction), Column 85: vertical discretization into 20 layers and the assigned K zones (according to Table 3); a vertical exaggeration factor of 2:1 is employed.

Fig. 5 - Sezione del dominio di modellazione lungo la traccia del tunnel (direzione N-S), Colonna 85: discretizzazione verticale in 20 layers e zone di K assegnate (secondo legenda di Tab. 3); esagerazione verticale di 2:1.

flow system were represented with the same b.c.: head values were assigned matching the riverbed elevations derived from the DEM. On the eastern side, the head ranged from 1045 to 520 m a.s.l. along the Devero River and from 520 to 300 m a.s.l. along the Toce River. On the western side, the head ranged from 1250 to 530 m a.s.l. along the Cairasca River and from 530 to 300 m a.s.l. along the Diveria River.

All cells outside the boundaries were deactivated, and the final shape of the domain was thus irregular. The 4 main springs were represented with the drain package (the 3rd type of b.c.), and a drain elevation value equal to the ground level in the spring was assigned to the cells. The conductance values, which were calibrated against the real flow rates of the springs, were 139.95 m²/d for the Lisiel spring, 55.45 m²/d for the Valle Oro spring, 1.11 m²/d for the Cesa spring and 7.65 m²/d for the Vegno spring.

The calibration process was implemented under steady-state conditions via simulations representing the present conditions and solved with the Link-algebraic MultiGrid solver package (Mehl and Hill 2001). The trial and error process (Zheng and Bennevy 1995) mainly determined the K values and uncertain b.c. types, i.e., a constant head at the northern boundary. All 17 piezometric control points were considered, for which at least one piezometric measurement was available. These data are provided in Table 5. The flow rates of the springs were considered to calibrate the conductance values.

The forecasting simulations were performed according to two tunnel behavior types: in the first type, representative of the drilling phase, the tunnel was assumed to be completely draining, while in the second type, representative of post-operam conditions, the tunnel was assumed to be dispersant.

The above draining tunnel was simulated with the drain package, which removes groundwater from cells in which the package is applied as a function of head differences (between the aquifer and tunnel elevations) and the conductance parameter near the tunnel. The drain elevation matched the tunnel elevation, while conductance (C) values (a parameter representing the resistance opposed to flow due to the rock

Tab. 5 - Calibration data for the simulation under ante-operam conditions.

Tab. 5 - Dati di calibrazione della simulazione ante-operam.

Spring name (ID)	Drain conductance	Observed values		Calculated values		Calculated - observed	Discrepancy
	m ² /d	L/s	m ³ /d	L/s	m ³ /d	m ³ /d	%
Lisiel (24)	139.95	34.96	3020.5	34.96	3020.2	-0.34	-0.01%
Valle Oro (23)	55.45	19.97	1725.4	19.97	1725.7	0.29	0.02%
Vegno (8)	7.65	1.55	133.9	1.5	130.0	-3.96	-2.96%
Cesa (22)	1.11	0.2	17.3	0.2	17.2	-0.03	-0.19%

mass surrounding the tunnel; Zaadnoordijk 2009) were calculated as:

$$C = \frac{(KPZ \cdot 2\pi R)}{h} \quad (4)$$

where KPZ is the hydraulic conductivity of the plastic zone, R is the tunnel radius and h is the plastic zone thickness.

Therefore, different C values were assigned to the tunnel reaches crossing rock mass zones with varying K values. Sensitivity analysis considered 3 KPZ values, assuming an increase of 5, 10 and 100 times the original rock mass K value.

Simulation of the dispersant tunnel considered an interior flow rate of 18 m³/s and calculated the resultant water exchange with the rock mass. The dispersant tunnel was represented by streamflow-routing package STR1 (Prudic 1989), and the 3rd type of b.c. was applied to simulate river-groundwater interactions, according to which the stream flow rate was propagated starting from the value in the most upstream cell (starting point) and calculated for each downstream cell as the previous flow rate plus or minus the stream flow rate gained from or lost to the aquifer. The in/out flow was calculated by multiplying the head difference between the stream and aquifer with the riverbed conductance. The water level within the tunnel occurred at 4 m above the tunnel bottom, while the conductance was calculated for the draining tunnel simulations.

Finally, other simulations were defined to evaluate the effects of concrete linings on the most critical sectors of the tunnel, thereby considering three K values for the plastic zone of the lining sectors: KPZ matching the K value for the drilled rock mass (A), KPZ = 0.1*K for the drilled rock mass (B), KPZ = 1E-07 m/s (C). In the sectors without linings, the KPZ value was 10 times the K value for the surrounding rock mass.

Results

Hydrogeological characterization and resulting conceptual model

The study area exhibits a temperate continental climate, characterized by a mean annual temperature of 11.3 °C in the city of Domodossola (Federici et al. 1967) and a mean annual rainfall ranging from 1250–2600 mm/year in the modeled area (variations are mainly related to the topographic elevation).

Two rainfall maxima occur every year: the first occurs in May (with values higher than 152 mm) and the second occurs in October/November (higher than 110 mm).

The water surplus in the modeled area was calculated to range from 700–1400 mm/year.

The resulting conceptual model indicated groundwater flow mainly controlled by gravity and a general aquitard behavior of the rock masses (mainly gneissic formations), except under tectonization, fracturing or dissolution conditions: the main aquifers are represented by metalimestones.

The spring survey revealed a higher density of springs with significant flow rates in the Crodo area and Alfenza valley (Fig. 6a).

Springs exhibited flow rates in a wide range: from 0.06 L/s (ID 21) to 35 L/s (ID 24 in Lisiel); the most representative flow rates ranged from 0.05–2.5 L/s. A clear correlation between the spring flow rate and spring elevation was not observed in the three main groups spatially distinguished: springs located at elevations between 400 and 500 m a.s.l. exhibited flow rates higher than 10 L/s (ID3 – Oira, ID23 – Valle Oro, ID24 – Lisiel); springs between 1100 and 1500 m a.s.l. exhibited flow rates ranging from 5 to 10 L/s (ID10 – Flecchio, ID12 – Longio, ID15 – Alfenza north); and the third group containing all remaining springs, located at variable elevations, exhibited flow rates lower than 5 L/s.

Comparing all the available data, it could be assessed that the springs with higher flow rates generally attained a low DVI, particularly the Valle Oro spring, which exhibited a relatively constant flow rate, independent of rainfall events, and a low value of the α coefficient (6.60E-03 d-1); this spring is representative of the end discharge of deep groundwater flow systems and is recharged across a large area.

Similar to nearby areas (Martinotti 1993), three hydrochemical water types occurred in the study area (Fig. 7a): Ca-HCO₃ facies, representative of relatively short and shallow flow pathlines circulating within gneiss rock masses or Quaternary deposits, such the Alfenza springs; Ca-SO₄ facies, representative of deep groundwater flow pathlines within gypsum and/or anhydrites in metalimestones (as demonstrated by the enrichment in sulfates), such as the Valle Oro spring and Molinetto well; Ca-HCO₃-SO₄ facies resulting from the mixing of the other two facies.

This classification was confirmed by the groundwater mineralization degree, which could be inferred from the specific electrical conductivity (EC), as shown in Figure 6b.

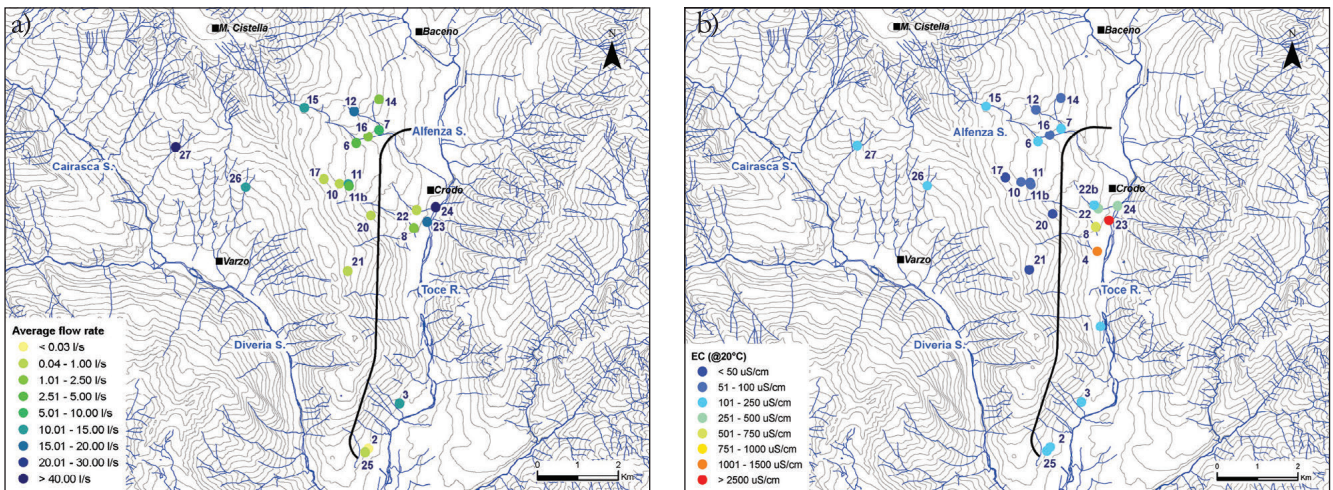


Fig. 6 - Location of the groundwater monitoring network: a) springs ranked as a function of the average flow rate during the period from Jul-05 to Jun-06; b) springs and wells ranked as a function of the average EC value during the same period.

Fig. 6 - Ubicazione della rete di monitoraggio delle acque sotterranee: a) sorgenti classificate in funzione della portata media sul periodo lug-05 – giu-06; b) sorgenti e pozzi classificate in funzione dell'EC media sullo stesso periodo.

Further coherent information was derived from analysis of groundwater samples collected in the boreholes at different depths: as shown in Figure 7b, the two deepest samples collected in the S3 borehole (CO_4 at 300 m b.g.l. and CO_5 at 376 m b.g.l.) exhibited the same facies of the Lisiel spring.

The isotopic composition of groundwater reflected the literature data quite well (Martinotti 1993; Martinotti et al. 1999; Pastorelli et al. 2001): the local meteoric line (Fig. 8a) was very similar to the global meteoric water line of Craig (1961). No significant thermal process occurred because no shifts in $\delta^{18}\text{O}\text{‰}$ were observed. The data remained within a

narrow $\delta^{18}\text{O}\text{‰}$ range, but the distribution was significant: the Cesa well corresponded to shallower and shorter flow pathlines and to a lower elevation of the recharge area, characterized by minor isotopic depletion; the Flecchio spring was similar to the Cesa well but located upstream and recharged at higher elevations; the Valle Oro spring was characterized by the most depleted waters and the largest difference between the theoretical recharge area average elevation and spring elevation (Fig. 8b), as this spring represents the discharge of deep and long flow pathlines.

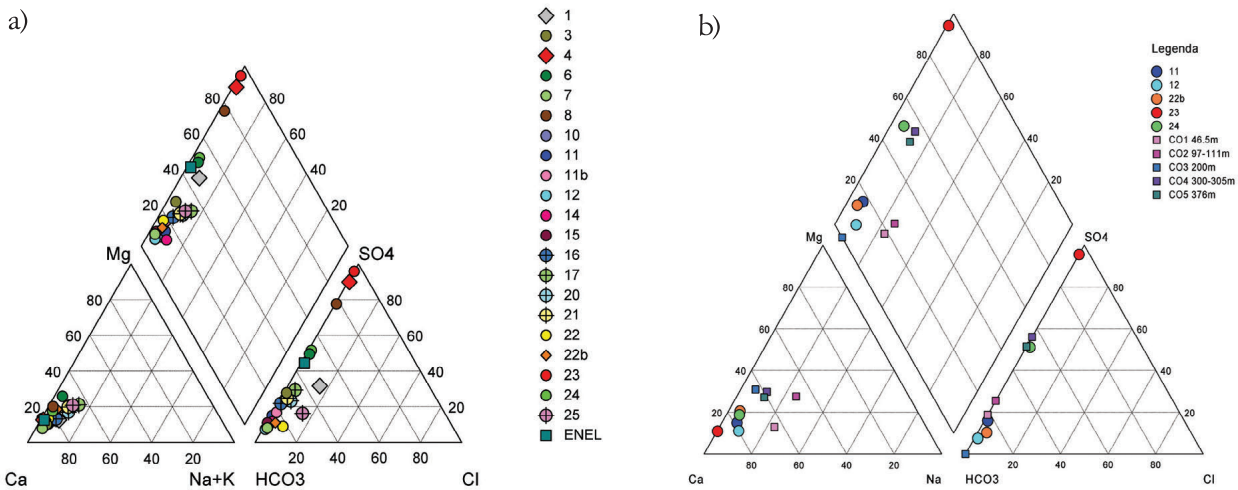


Fig. 7 - Piper diagrams: a) all monitoring points in the study area; b) five groundwater samples collected in borehole S3 compared to the four main monitored springs.

Fig. 7 - Diagrammi di Piper: a) tutti i punti di monitoraggio sull'area di studio; b) cinque campioni di acque sotterranee raccolti al sondaggio S3, comparati con le quattro sorgenti principali.

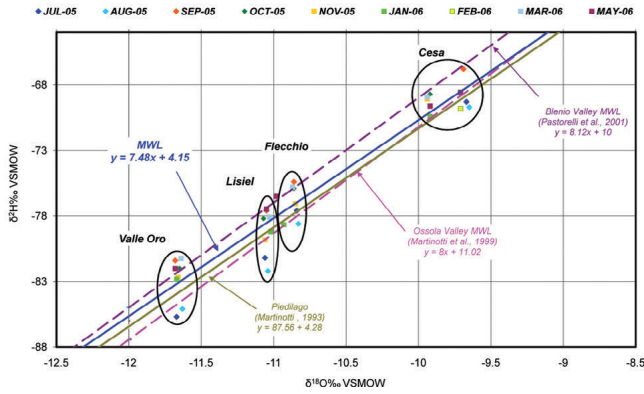


Fig. 8a - Local meteoric water line derived from all the available data on the study area.

Fig. 8a - Linea meteorica locale derivata da tutti i dati disponibili sull'area di studio.

Risk evaluation results obtained with the parametric methods

The final result in terms of the potential inflow (PI), expressed as a probability between 0% and 100%, for the entire tunnel is shown in Figure 9. Most critical sectors included those between 6+062 km and 6+864 km, located below the DSGD, where the PI value (between 40–60% and 60–80%) was mainly controlled by FF (RQD), with a rating of 0.75. Other critical sectors occurred at 177 and 178 (8+867–8+917 km), where the high rating of the RQD index, OV (approximately 120 m) and K contributed to a higher PI value. The remainder of the tunnel exhibited PI values in the range from 0-40%.

The final results according to the Cesano method in terms of the major and minor inflows are shown in Figures 10 and 11, respectively. The most critical sectors in terms of the major inflows, with values between 80% and 100%, were related to the lineament occurrence and location of the ground surface and bedrock troughs. Concerning seepage and minor inflows, the most critical sectors were located in the northern half of the tunnel, where in certain sectors, the maximum value of a 100% probability was attained.

Observing Figures 9 and 10 and comparing the results of these two methods, it was evident that the PI value distribution along the tunnel was quite diversified. On average, lower PI values were produced by the Dematteis method. Nevertheless, the authors considered these results more reliable for two reasons: this method is more codified than is the Cesano method within the involved geological framework, and this method is strongly based on rock mass intrinsic parameters. The Cesano method for major inflow prediction mainly considers morphological and geological factors, which do not play a key role under the thick overburden observed at the investigated site.

The frequency histogram of the Dematteis PI results (Fig. 12) reveals a typical lognormal distribution, as expected if we consider the output of a combination of hydrogeological factors; the modal class corresponds to a very low PI value (15%), as usually observed in regard to the actual drainage

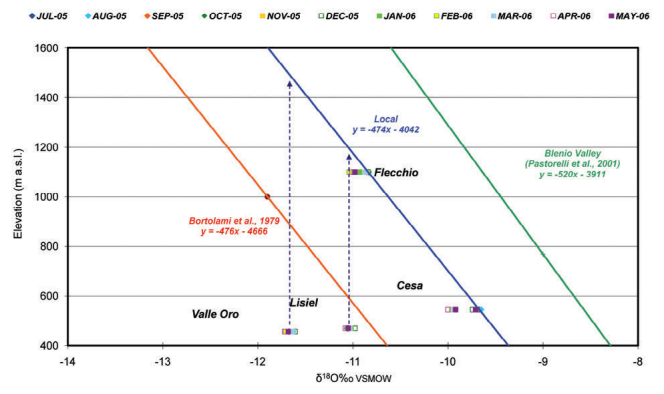


Fig. 8b - Relationship between spring elevation and $\delta^{18}O‰$.

Fig. 8a - Relazione tra la quota della sorgente e $\delta^{18}O‰$.

distribution occurrence in bored tunnels (Masset and Loew 2010). In hard rock aquifers, high inrush events are sporadic, and scattered drainage events rarely occur with respect to groundwater seepage from the excavated tunnel surface (Gargini et al. 2008). Additionally, for this reason, the Dematteis output appeared more reliable than did the Cesano method output.

The DHI value for all springs (and for the 5 wells, considered as water points potentially subject to impact), according to the application of the Dematteis method, is reported in Table 7 as DHID; it is important to emphasize that the DHID value

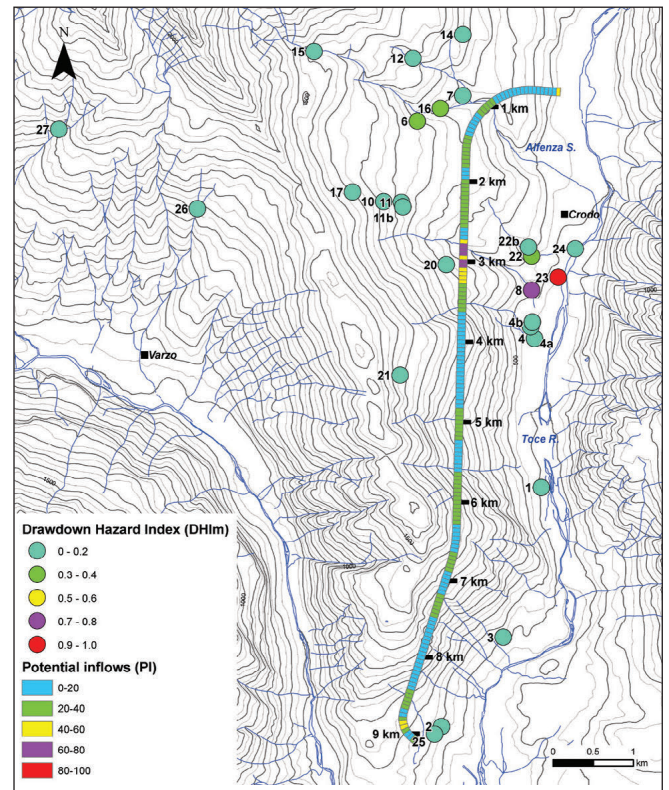


Fig. 9 - Potential inflows within the tunnel according to the Dematteis method and modified drawdown hazard index (DHIM) at the water points (springs and wells).

Fig. 9 - Venute idriche potenziali in galleria in base al metodo Dematteis e Drawdown Hazard Index modificato (DHIM) ai punti d'acqua (sorgenti e pozzi).

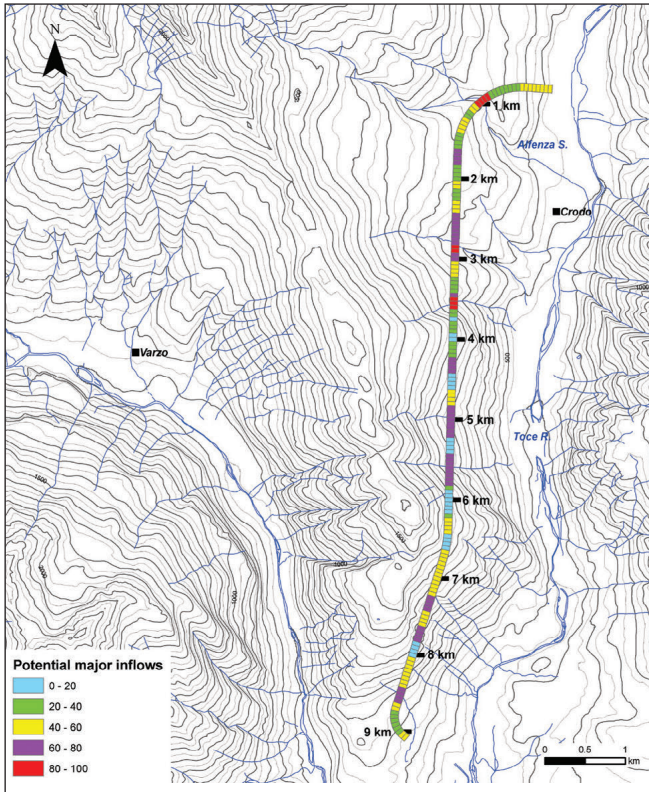


Fig. 10 - Potential major inflows within the tunnel according to the Cesano method.

Fig. 10 - Potenziali venute idriche primarie in galleria secondo il metodo Cesano.

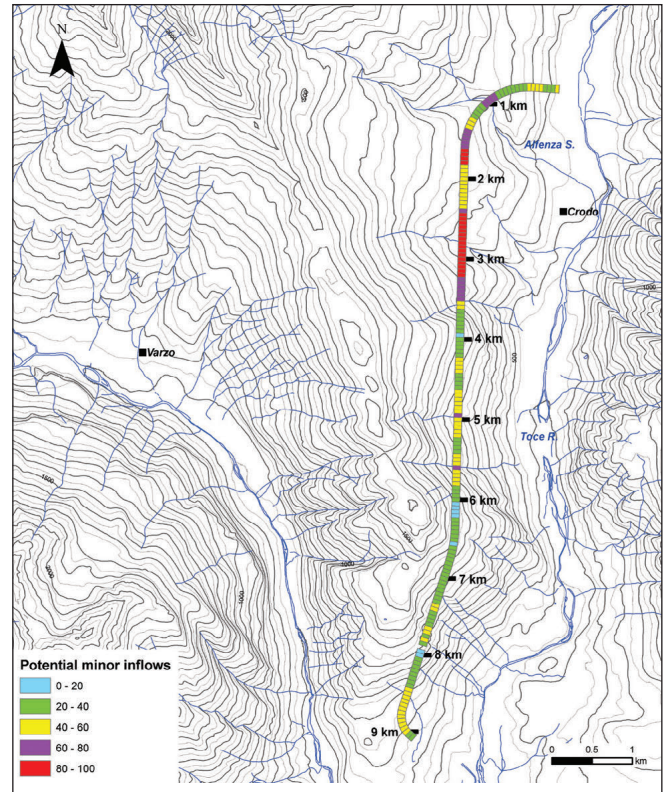


Fig. 11 - Potential minor inflows within the tunnel according to the Cesano method.

Fig. 11 - Potenziali venute idriche secondarie in galleria secondo il metodo Cesano.

never reaches 0, as conditioned by the PI value, but always remains higher than 0.23. Therefore, the absence of DHI probability occurrence does not occur. Springs with higher DHI values include ID 23 (Valle Oro; 0.91 DHI) and ID 8 (Vegno; 0.68 DHI), both located near a main fault crossing the tunnel and connected to deep groundwater flow systems.

If the DHID values were ranked in classes based on the limits originally proposed by the Dematteis method (Table 1), then only 1 spring would occur in classes 1 and 2 (Valle Oro and Vegno, respectively), whereas the remaining 19 springs and 5 wells would occur in the partial risk class (DHID >0.23). Among these springs and wells, 10 springs (and 1 well, the Sarizzo Well) exhibited the minimum DHID value of 0.23; as already mentioned, a value of 0.23 is derived simply from the fact that PI is always positive. This consideration reveals a limitation of the methodology: springs located relatively far from the tunnel path, connected to a shallow groundwater flow system or unrelated to any tectonic lineament, e.g., a receptor with a very low vulnerability (if any), will not, however, be assigned a fair DHID value, which is largely controlled by PI.

If the PI value is high, accordingly, the DHID value will at least reach a moderate level for all springs involved in the evaluation. For this reason, the Dematteis method tends to overestimate the impact risk for springs with a low hydrogeological vulnerability. The DHID estimation method is more reliable for medium-high vulnerability receptors.

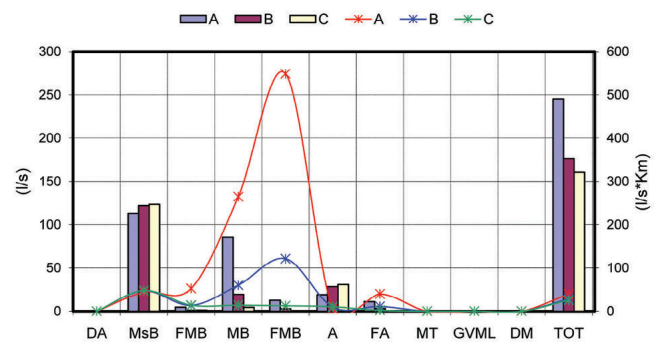


Fig. 12 - Total forecasted tunnel outflow (bars, left scale) and specific outflow normalized by the distance (line, right scale) in relation to the lithology (DA = Quaternary fluvial deposits; MsB = Baceno micascists; FMB = fault zones in the Baceno micascists; MB = Baceno metasediments; FMB = fault zones in the Baceno metasediments; A = Antigorio Gneiss; FA = fault zones in the Antigorio Gneiss; MT = Teggiolo metasediments; GVML = Valgrande and Monte Leone Gneiss; DM = Glacial deposits; TOT = Totali).

Fig. 12 - Previsione della portata totale drenata dalla galleria (barre, asse y di sinistra) e della portata specifica normalizzata sulla distanza (linee, asse y di destra) in relazione alla litologia (DA = depositi fluviali quaternari, MsB = Micascisti di Baceno, FMB = zone di faglia in Micascisti di Baceno, MB = Metasedimenti di Baceno, FMB = zone di faglia in Metasedimenti di Baceno, A = Gneiss di Antigorio, FA = zone di faglia in Gneiss di Antigorio, MT = Metasedimenti di Teggiolo, GVML = Gneiss di Valgrande e Monte Leone, DM = depositi glaciali, TOT = Totali).

Considering these limitations and other improvements of a hydrogeological nature based on previous experience derived from tunnels drilled in hard rock aquifers, the final drawdown index was slightly modified by defining a new index, namely, the modified DHI (DHIM; Table 6). DHIM was evaluated in the same manner to DHID with the following rules:

1. If the tunnel-spring Euclidean distance is larger than 1000 m and there is no evidence of a hydrogeological connection with the tunnel, a DHID value of 0 is assumed, notwithstanding the PI value; this consideration is based on the results of hydrogeological monitoring of the springs and wells along the pathway of the Florence-Bologna high-speed railway tunnel connection (Canuti et al. 2009);
2. If the tunnel-spring Euclidean distance is smaller than 1000 m and there is no evidence of a hydrogeological connection with the tunnel, DHID is assumed to be based on the average PI relative to the tunnel sector included within a buffer radius of 1000 m centered at the spring;
3. If the tunnel-spring Euclidean distance is smaller than 1000 m and there is evidence of a hydrogeological connection with the tunnel, two separate buffer zones are considered: a sphere with a 1000-m radius centered at the spring and a 400-m long tunnel sector across the fault-tunnel intersection; the highest value of PI between these buffer zones is conservatively chosen to calculate DHI at the spring;
4. If the tunnel-spring Euclidean distance is larger than 1000 m and there is evidence of a hydrogeological connection with the tunnel (with a total connection distance along the faults smaller than 2000 m), a 400-m long tunnel sector buffer zone across the fault-tunnel intersection is defined for PI evaluation;
5. The obtained DHI value is normalized to 1, and all values are ranked according to 5 equally spaced classes between 0 and 1. The normalized DHI is referred to as the modified DHI (DHIM).

The final DHIM result for the whole set of receptors is shown in Fig. 9. A comparison between the DHID and DHIM class ranking results is presented in Table 7.

Tab. 6 - DHI values for all springs according to the application of the Dematteis method; 1 = highest, 5 = lowest impact probability.

Tab. 6 - Valori DHI per tutte le sorgenti secondo il metodo Dematteis; 1= valori massimi, 5 = valori minimi della probabilità d'impatto.

ID	Name	DHID	DHID CLASS	DHIM	DHIM CLASS
1	SARIZZO WELL	0.23	3	0	5
2	BISOGNO	0.23	3	0.11	5
10	FLECCHIO ALTA	0.23	3	0	5
11	FLECCHIO	0.23	3	0.14	5
11b	FLECCHIO ISOLATA	0.23	3	0.13	5
15	ALFENZA NORD	0.23	3	0	5
17	CAVORAGA - FAIO'	0.23	3	0.198	5
21	CHEGGIO	0.23	3	0	5
25	LA CONCA	0.23	3	0.11	5
26	LA ROCCA	0.23	3	0	5
27	CALANTAGINE	0.23	3	0	5
24	LISIEL	0.34	3	0	5
3	OIRA	0.46	3	0.07	5
4	MOLINETTO 1	0.46	3	0.09	5
4a	MOLINETTO 2	0.46	3	0.13	5
4b	MOLINETTO 3	0.46	3	0.14	5
6	VICENO	0.46	3	0.31	4
7	LA VALLE	0.46	3	0.08	5
12	LONGIO	0.46	3	0.16	5
14	TRONA	0.46	3	0.16	5
16	ALFENZA SUD	0.46	3	0.22	4
22	CESA INFERIORE	0.46	3	0.37	4
22b	CESA WELL	0.46	3	0.18	5
8	VEGNO	0.68	2	0.75	2
23	VALLE ORO	0.91	1	1	1
20	RONCONI	0.55	3	0.6	3→5

Tab. 7 - Impacts on the springs forecasted via MODFLOW simulations with the draining tunnel and 3 K values for the plastic zone.

Tab. 7 - Impatti sulle sorgenti previsti attraverso le simulazioni MODFLOW con galleria drenante e con i 3 diversi valori di K applicati alla zona plastica.

	Lisiel (24)	Valle Oro (23)	Vegno (8)	Cesa (22)	
Observed	34.96	19.97	1.55	0.2	Q (L/s)
Ante-operam	34.96	19.97	1.5	0.2	Q (L/s)
Post (1/2 order)	33.56	18.92	0	0	Q (L/s)
	4.00%	5.25%	100%	100%	deficit %
Post (1 order)	33.47	18.9	0	0	Q (L/s)
	4.25%	5.39%	100%	100%	deficit %
Post (2 order)	33.37	18.82	0	0	Q (L/s)
	4.53%	5.77%	100%	100%	deficit %
Average deficit %	4.26%	5.47%	100%	100%	deficit %

Tunnel inflows and spring dewatering forecasted with the numerical model

The numerical simulations with the completely draining tunnel predicted piezometric drawdowns ranging from 200–800 m, depending on the K values assigned to the plastic zone around the tunnel.

In all the simulations, the highest drawdown occurred above the tunnel at the large fold close to the northern entrance (around km 1) and progressively decreased from north to south along the longitudinal direction of the tunnel; drawdown caused where the tunnel elevation was higher than the piezometric surface under natural conditions. Along the transversal direction (W-E), the depressurization effect progressively decreased away from the tunnel axis and disappeared at a maximum distance of approximately 5 km on the west side.

In all three simulations, piezometric drawdown caused drying of the two springs located in the area of the maximum impact (Cesa and Vegno). At the other two springs (Lisiel and Valle Oro), located in the same area but at lower elevations than those of the previous ones, the model forecasted a flow rate decrease in the 4–6% range (Tab. 8).

In the three simulations, the total tunnel drainage under steady-state conditions reached 273, 286 and 316 L/s.

The highest contribution stemmed from the Baceno metasediments, which resultant flow rates ranging from 100–115 L/s (i.e., accounting for 31.6–42% of the total drainage). Progressively minor contributions originated from the remaining hydrogeological units and related fault zones: Baceno micaschists, fault zones in the Baceno metasediments, fault zones in the Antigorio Gneiss, Antigorio Gneiss and fault zones in the Baceno micaschists (Tab. 9).

Considering the inflow normalized by the tunnel length, the sectors crossing the faults in the Baceno metasediments exhibited the highest values, from 0.833 to 1.215 L/s*m; these values progressively decreased in the following order: Baceno metasediments, fault zones in the Baceno micaschists,

Baceno micaschists, fault zones in the Antigorio Gneiss and Antigorio Gneiss. These results mainly stemmed from the assigned hydraulic conductivity values and from the geometric position of the units with respect to the piezometric surface and tunnel alignment.

In the three simulations of the dispersant tunnel (with an interior flow rate of 18 m³/s), the tunnel still exhibited draining behavior located below the piezometric surface, while the aquifer located above the piezometric surface was recharged.

This led to a slight decrease in terms of the depressurization effect in the area of the highest impact; at springs Lisiel and Valle Oro, the flow rates increased by 0.01 and 0.28 L/s, respectively, with respect to the simulations of the draining tunnel, while at springs Vegno and Cesa, the impact remained the same (Tab. 10).

Finally, the last three simulations, with impermeable linings in the most permeable tunnel reaches, demonstrated that linings effectively reduced depressurization in terms of the intensity and area of influence. Along the tunnel, maximum drawdowns decreased by more than half with respect to the corresponding values calculated in the first simulation involving the completely draining tunnel (~350 m of drawdown), resulting in 153 m under scenario A, 140 m under scenario B, and 138 m under scenario C. The flow rates at springs Lisiel and Valle Oro decreased by 2% and 4.5%, respectively, with respect to the values under natural conditions. The Cesa spring was greatly impacted under all the scenarios, while the Vegno spring completely dried only under the A scenario. In contrast, under the B and C scenarios, the Vegno spring exhibited a flow rate decrease of 82% and 64%, respectively, with respect to the natural-condition values (Table 11). The total tunnel drainage also decreased significantly: 245 L/s (A), 176 L/s (B) and 161 L/s (C).

The general effect of tunnel sealing was quite good, even this measure increased drainage along the tunnel reaches without linings, due to the high hydraulic gradient (Table 12 and Fig. 12).

Tab. 8 - Tunnel inflows forecasted by the MODFLOW simulations, according to the 3 scenarios described in the main text; the tunnel reaches crossing the different hydrogeological units are distinguished to calculate linear flow rates (every m or km of tunnel advancement).

Tab. 8 - Venute idriche in galleria previste attraverso le simulazioni MODFLOW, sui 3 scenari descritti nel testo; i tratti di galleria che attraversano le diverse unità idrogeologiche sono distinti per poter calcolare le portate lineari (ogni m o km di avanzamento dello scavo).

Zone Budget	Hydrogeological Unit	Post (1/2 order)		Post (1 order)		Post (2 order)	
		Q (L/s)	Q (L/s*Km)	Q (L/s)	Q (L/s*Km)	Q (L/s)	Q (L/s*Km)
6	Quaternary fluvial deposits	0	0	0	0	0	0
7	Baceno micaschists	90.83	35.05	105.01	40.52	155.81	60.12
8	Fault in Baceno micaschists	14.44	164.91	14.58	166.44	15.99	182.51
9	Metasediments (Baceno syncline)	114.84	356.15	116.57	361.54	100.08	310.38
10	Fault in Metasediments (Baceno syncline)	27.61	1214.81	23.8	1047.26	18.94	833.31
11	Antigorio gneiss	12.5	4.39	12.85	4.63	13.08	4.76
12	Fault in Antigorio gneiss	12.75	46.17	12.82	46.43	12.33	44.62
13	Metasediments (Teggiolo syncline)	0	0	0	0	0	0
14	Valgrande and Monte Leone gneiss	0	0	0	0	0	0
15	Quaternary glacial deposits	0	0	0	0	0	0
	Total and average	272.97	44.2	285.64	46.82	316.22	52.04

Tab. 9 - Impacts on the spring flow rates forecasted by the model simulations involving the draining tunnel (Post) and dispersant tunnel (Stream).

Tab. 9 - Impatti sulle portate delle sorgenti previsti dalle simulazioni modellistiche con galleria drenante (post) e galleria disperdente (Stream).

	Lisiel (24)	Valle Oro (23)	Vegno (8)	Cesa (22)	
Observed	34.96	19.97	1.55	0.2	Q (L/s)
Ante-operam	34.96	19.97	1.5	0.2	Q (L/s)
Stream (1/2 order)	33.75	19.07	0	0	Q (L/s)
	3.46%	4.54%	100%	100%	deficit %
Stream (1 order)	33.6	19	0	0	Q (L/s)
	3.87%	4.90%	100%	100%	deficit %
Stream (2 order)	33.45	18.83	0	0	Q (L/s)
	4.30%	5.72%	100%	100%	deficit %
	3.88%	5.05%	100%	100%	average deficit %

Tab. 10 - Impacts on the spring flow rates forecasted by the model simulations involving the draining tunnel (Post 1 order) and sealed tunnel (linings prevent major groundwater inflows; please refer to the main text for more detail).

Tab. 10 - Impatti sulle portate delle sorgenti previsti dalle simulazioni modellistiche con galleria drenante (post 1 order) e con galleria impermeabilizzata (rivestimenti applicati in corrispondenza delle venute idriche primarie, spiegazione nel testo).

	Lisiel (24)	Valle Oro (23)	Vegno (8)	Cesa (22)	
Observed	34.96	19.97	1.55	0.2	Q (L/s)
Ante-operam	34.96	19.97	1.5	0.2	Q (L/s)
Post 1 order	33.56	18.92	0	0	Q (L/s)
	4.00%	5.25%	100%	100%	deficit %
A scenario	33.73	19.07	0	0	Q (L/s)
	3.52%	4.52%	100%	100%	deficit %
B scenario	34.12	19.39	0.27	0	Q (L/s)
	2.38%	2.90%	82.10%	100%	deficit %
C scenario	34.23	19.48	0.55	0	Q (L/s)
	2.09%	2.46%	63.64%	100%	deficit %
	2.66%	3.29%	81.91%	100%	average deficit %

Tab. 11 - Tunnel inflows forecasted by the MODFLOW simulations, according to the 3 scenarios involving the sealed tunnel (as described in the main text); the tunnel reaches crossing the different hydrogeological units are distinguished to calculate linear flow rates (every km of tunnel advancement).

Tab. 11 - Venute idriche previste dalle simulazioni MODFLOW sui 3 scenari con la galleria impermeabilizzata (spiegazione nel testo); i tratti di galleria che attraversano le diverse unità idrogeologiche sono distinti per poter calcolare le portate lineari (ogni m o km di avanzamento dello scavo).

Zone Budget	Hydrogeological Unit	Scenario A		Scenario B		Scenario C	
		Q (L/s)	Q (L/s*Km)	Q (L/s)	Q (L/s*Km)	Q (L/s)	Q (L/s*Km)
6	Quaternary fluvial deposits	0	0	0	0	0	0
7	Baceno micashists	113.18	43.67	121.84	47.01	123.4	47.62
8	Fault in Baceno micashists	4.58	52.28	1.17	13.31	1.2	13.75
9	Metasediments (Baceno syncline)	85.32	264.61	19.33	59.93	4.43	13.74
10	Fault in Metasediments (Baceno syncline)	12.47	548.63	2.75	121.06	0.28	12.37
11	Antigorio gneiss	18.87	6.5	28.22	9.48	30.66	10.22
12	Fault in Antigorio gneiss	10.91	39.51	3.03	10.97	0.56	2.01
13	Metasediments (Teggiolo syncline)	0	0	0	0	0	0
14	Valgrande and Monte Leone gneiss	0	0	0	0	0	0
15	Quaternary glacial deposits	0	0	0	0	0	0
	Total and average	245.33	39.4	176.33	27.98	160.54	25.38

Tab. 12 - Forecasted spring impact scenarios according to the parametric (DHI) and numerical (MODFLOW) models. Please refer to the text for the definition of the global risk classes.

Tab. 12 - Scenari d'impatto previsti sulle sorgenti secondo i modelli parametrico (DHI) e numerico (MODFLOW). Vedere il testo per la definizione delle classi di rischio globale.

Spring - well	DHI Dematteis modified	MODFLOW	Risk class
23-Valle Oro	●	●	●
8 - Vegno	●	●	●
22 - Cesa Inferiore	●	●	●
6 - Viceno	●		●
16 - Alfenza Sud	●		●
17 - Carovaga-Faiò	●		●
20 - Ronconi	●		●
22B - Pozzo Cesa	●		●
14 - Trona	●		●
12 - Longio	●		●
11 - Flecchio	●		●
4B - Molinetto 3	●		●
11B - Flecchio Isolata	●		●
4A - Molinetto 2	●		●
25 - La Conca	●		●
2 - Bisogno	●		●
4 - Molinetto 1	●		●
7 - La Valle	●		●
3 - Oira	●		●
27 - Calantagine	●		●
26 - La Rocca	●		●
24 - Lisiel	●	●	●
21 - Cheggio	●		●
15 - Alfenza Nord	●		●
10 - Flecchio Alta	●		●
1 - Pozzo Sarizzo	●		●

Risk class

- Very high risk
- High risk
- Low risk
- Medium risk
- Minimum risk - No risk

Comparison of the two methods

Before comparing the parametric and numerical modeling approaches, it should be noted that both evaluation methods of tunnel impacts are based on detailed construction of a geological model and a dedicated geological survey. A site-specific direct survey is the essential prerequisite for dependable impact evaluation, regardless of the chosen approach.

In every approach, the conservativity principle was always followed, e.g., determination of the thickness of the plastic zone or modeling under steady-state conditions.

However, the reliability of the forecasted scenarios is limited by the calibration dataset (hydraulic head and spring monitoring and pumping test data).

As indicated in Table 12, the final results in terms of tunnel impact forecasts are reported. The impact scenario is relative to the draining tunnel under steady-state conditions. The resulting risk classes indicate the probability and severity of the impact occurrence retrieved from the parametric (DHIM evaluation) and numerical evaluation processes, respectively.

Four risk classes are indicated in color from red (class I) to blue (class IV); in the third column of Table 12, the final output of the integrated tunnel impact evaluation is provided. The final choice was based as follows: if, for a given spring, the parametric and numerical methods produced 2 risk classes separated by an intermediate class, the last class was designated as the final output, thus recognizing similar uncertainties in both methods; if the parametric and numerical methods produced 2 contiguous risk classes for the same spring, the worst class was adopted as the final output given the principle of conservativeness.

Excavation and consequent drainage of the Crevola Toce diversion tunnel could yield the following expected scenarios of impact considering the main hydrogeological receptors:

- a medium risk for the Valle Oro spring: a very high probability (91%) of a 5% reduction in the average annual flow rate (the risk was ranked as medium because the probability was high according the DHIM output, but discharge depletion was poor);
- a medium risk for the Vegno spring: a high probability (68%) of a 31% reduction in discharge;
- a medium risk for the Cesa spring: a medium probability (46%) of complete drying;
- a medium–low risk for the Lisiel spring: a low probability (34%) of a 6% discharge reduction;
- a medium–low risk for the Molinetto wells: a medium probability (46%) of well yield reduction;
- a medium–low risk for the Oira, Viceno, La Valle, Trona, Alfenza Sud, and Longio springs and the Cesa well: a medium probability (46%) of impact;
- a low risk for the remainder of the receptors: a low impact probability (23%) under shallow groundwater flow systems. Additionally, the Ronconi spring was assigned to this last class, independent of the DHIM output, because this spring is representative of a shallow groundwater flow system at an elevation much higher than the tunnel elevation.

Conclusions and remarks

An evaluation method of the tunnel drainage impact risk considering hydrogeological receptors was presented and examined. To overcome the intrinsic uncertainty in forecasting under ante-operam conditions and to strengthen

the evaluation, a rating- and weighting-based parametric method and numerical model were contemporarily applied. The results were compared, and a final forecast result was obtained upon result combination via a conservative approach.

These two methods revealed their respective limits and advantages. Parametric methods do not consider the groundwater flow equation but allow us to easily assess the risk probability for all springs. Another advantage is that these methods can be adapted to a given case study as a function of the available input data. Nevertheless, the obtained approximate results require critical evaluation and refinement. In contrast, numerical modeling requires more data (hydraulic heads and flows), and the reliability greatly depends on the data quantity and quality and on the effectiveness of the calibration process. However, the modeling process allows conceptual model assessment by applying the groundwater flow equation.

In the specific case study, the peculiarity and strength of the available dataset involved the application of different field methods (geological surveys, flow and piezometric measurements, hydrochemistry analysis, and isotopic techniques), greatly promoting conceptual model establishment. The dataset was sufficiently detailed for the application of parametric methods but still insufficient for the numerical modeling process. Furthermore, the model setup required a notable effort due to the geological complexity and steep slopes.

Based on the experience obtained with the presented case study, it is suggested to first employ parametric methods as a first-level risk evaluation of all the water points to assess the most vulnerable locations. Then, considering these vulnerable points, a second-level risk evaluation should be conducted via numerical modeling based on a highly detailed hydrogeological dataset.

Acknowledgement

Presented at Session "Hydrogeological impacts of tunnels", GEOITALIA 2009, Rimini, September 2009 (session's conveners: Alessandro Gargini, Valentina Vincenzi, Michele Sapigni).

Competing interest

The authors declare no competing interest.

Additional information

Supplementary information is available for this paper at <https://doi.org/10.7343/as-2022-558>

Reprint and permission information are available writing to acquessotterranee@anipapozzi.it

Publisher's note Associazione Acque Sotterranee remains neutral with regard to jurisdictional claims in published maps and institutional affiliations.

REFERENCES

- Aller L, Bennett T, Lehr JH, Petty RJ (1985) DRASTIC - a standardized system for evaluating ground water pollution potential using hydrogeologic settings: U.S. Environmental Protection Agency, Robert S. Kerr Environmental Research Laboratory, Office of Research and Development, EPA/600/2-85/018, 163 pp.
- Astolfi G, Sapigni M (1999) Impianto Crevola Toce III - Progetto di Massima - Relazione geologica "Crevola Toce III Plant - Preliminary Design - Geological Report". Enel Spa, internal report.
- Barton CM (1974) Engineering classification of rock masses for the design of tunnel support. *Rock Mechanics*, 6, 4, pp.189-239.
- Bigioggero B, Boriani A, Origoni Giobbi E (1977) Microstructure and mineralogy of an Orthogneiss (Antigorite Gneiss - Lepontine Alps). *Rendiconti Società Italiana di Mineralogia e Petrologia*, 33, 99-108.
- Bistacchi A, Massironi M (2000) Post-nappe brittle tectonics and kinematic evolution of the north-western Alps: an integrated approach. *Tectonophysics*, 327, 267-292.
- Bortolami GC, Ricci B, Sella GF, Zuppi GM (1979) Isotope hydrology of the Val Corsaglia, Maritime Alps, Piedmont, Italy, in *Isotope Hydrology 1978, Vol.I, IAEA Symposium 228, June 1978, Neuheberg, Germany*, pp. 327-350.
- Campani M, Mancktelow N, Seward D, Rolland Y, Müller W, And Guerra I (2010) Geochronological evidence for continuous exhumation through the ductile-brittle transition along a crustal-scale low-angle normal fault: Simplon Fault Zone, central Alps. *Tectonics*, 29, TC3002, doi:10.1029/2009TC002582.
- Canuti P, Ermini L, Gargini A, Martelli L, Piccinini L, Vincenzi V (2009) Le gallerie TAV attraverso l'Appennino toscano: impatto idrogeologico ed opere di mitigazione "The High Velocity tunnels through the Tuscan Apennine: hydrogeological impact and mitigation strategies". Edifir-Edizioni Firenze, Firenze, pp. 207.
- Castiglioni GB (1958) Studio geologico e morfologico del territorio di Baceno e Premia "Geological and morphological study of the Baceno and Premia territory". *Memorie degli Istituti di Geologie e Mineralogie dell'Università di Padova*, vol. XX, 2-82.
- Cesano D, Olofsson B, Bagtzoglou (2000) Parameters regulating groundwater inflows into hard rock tunnels—a statistical study of the Dolmen tunnel in southern Sweden. *Tunneling and underground Space Technology*, V. 15/2, p. 153-165
- Civita M (1973) Schematizzazione idrogeologica delle sorgenti normali e delle relative opere di captazione "Hydrogeological sketch of normal springs and their capture works". In *Memorie e Note Ist. Geol. Appl. Napoli*, 12, 1973, pp.1-34.
- Civita M, De Maio M (2000) Valutazione e cartografia automatica degli acquiferi all'inquinamento con il sistema parametrico SINTACS R5 "Evaluation and automatic cartography of aquifers vulnerability to pollution with the parametric method SINTACS R5" Pitagora Editore, Bologna, 275pp.
- Civita M (2005) - Idrogeologia applicata e ambientale "Applied and environmental hydrogeology". Casa Editrice Ambrosiana, pp 331-336.
- Civita M, Gargini A, Pranzini G (1999) Metodologia di redazione della carta della vulnerabilità intrinseca e del rischio di inquinamento degli acquiferi del Valdarno Medio "Mapping methodology of intrinsic vulnerability and pollution risk for the Valdarno Medio aquifers". *Quaderni di Geologia Applicata*, 2, Vol.1, Pp. 1.59-1.73.
- Clark I, Fritz P (1997) *Environmental Isotopes in Hydrogeology*, CRC Press LLC.
- Craig H (1961) Isotopic variations in meteoric waters. *Science*, 133, pp. 1702-1703.
- Deere DU, Deere DW (1989) Rock Quality Designation (RQD) After Twenty Years - Technical Report GL-89-1, U.S. Army Engineer Waterways Experiment Station, Vicksburg, MS 39180.
- Deere DU, Merritt AH, And Coon RF (1969) "Engineering Classification Of In Situ Rock" - Air Force Systems Command, Kirtland Air Force Base, Report AFWL-64-144.

- Dematteis A, Kalamaras G, Eusebio A (2001) "A system approach for evaluating springs drawdown due to tunneling" - AITES-ITA 2001 World Tunnel Congress: Progress in tunnelling after 2000 - p. 257-264. Milano, 10-13 June 2001
- Domenico P, Schwartz F (1998), "Physical and chemical Hydrogeology", second edition. John Wiley & Sons, Inc., New York, USA
- Einstein HH (1988) "Special lecture: landslide risk assessment procedure" - Atti di "V International Symposium on Landslides", Losanna, 2, pp.1075-1090.
- Federici P C, Saccani F, Parietti P 1967 Le acque salutarie della Val d'Ossola "*The healthy waters of Val d'Ossola*". Collana di monografie dell'ateneo parmense, n. 18.
- Federico F (1984) Il processo di drenaggio da una galleria in avanzamento "*The drainage process from an advancing tunnel*". Rivista Italiana di Geotecnica, V.4, p. 191-208.
- Gargini A, Piccinini L, Martelli L, Rosselli S, Bencini A, Messina A, Canuti P (2006) Idrogeologia delle unità torbiditiche: un modello concettuale derivato dal rilevamento geologico dell'Appennino Tosco-Emiliano e dal monitoraggio ambientale per il tunnel alta velocità ferroviaria Firenze-Bologna "*Hydrogeology of turbidite units: a model conceptual derived from the geological survey of the Tosco-Emiliano Apennines and environmental monitoring for the tunnels of Florence-Bologna high speed railway line*". Bollettino Società Geologica Italiana, 125 (2006), 293-327.
- Goodman RE, Moye D, Schalkwyk A, Javandel I. (1965) "Groundwater inflows during tunnel driving." - Geol. Soc. America Publication - Engineering Geology, V. 2, p. 39-56.
- Grasemann B, Mancktelow N (1993) Two-dimensional thermal modelling of normal faulting: the Simplon Fault Zone, Central Alps, Switzerland. Tectonophysics, 225, 155-165.
- Grosjean G, Sue C, Burkhard M (2004) Late Neogene extension in the vicinity of the Simplon fault zone (central Alps, Switzerland). Eclogae geol. Helv., 97; 33-46.
- Harbaugh AW, Banta ER, Hill MC, McDonald G (2000) MODFLOW-2000, The U.S. Geological Survey modular groundwater model - User Guide to modularization concepts and the ground-water flow process - U.S. Geological Survey, Open-File Report 00-92
- Kanit T, Forest S, Galliet I, Mounoury V, Jeulin D. (2003) Determination of the size of the representative volume element for random composites: statistical and numerical approach. International Journal of Solids and Structures, 40, 3647-3679.
- Jiao Y, Hudson JA (1995) "The Fully-Coupled Model for Rock Engineering Systems." - International Journal of Rock Mechanics and Mining Sciences & Geomechanics Abstracts, 32, (5), 491-512. Oxford, United Kingdom: Elsevier Science)
- Lei S (1999) "An analytical solution for steady state flow into a tunnel." Ground Water - V. 37/1, p. 23-26.
- Lei S (2000) "Steady state flow into a tunnel with constant pressure boundary". Ground Water V.38/5, p. 643-644.
- Leopold LB Et Al (1971) "A procedure for evaluating environmental impact", U.S. Geological Survey Circular 645, Washington D.C., U.S. Dep. Of the Interior.
- Loew S (2002) In Barla G & Barla M (EDS) Le opere in sotterraneo e il rapporto con l'ambiente "*Underground works and their relation with environment*" - IX ciclo MIR, Torino 26-27 novembre 2002, Patron Editore, p. 201-217.
- Long JCS, Remer JS, Wilson CR, Witherspoon PA (1982) Porous Media Equivalent for Networks of Discontinuous Fractures. Water Resources Research, 18(3), 645-658.
- Maillet E (1905) Essais d'hydraulique souterraine et fluviale "*Evaluations on underground and river hydraulic*". Librairie Sci. Hermann Paris, 218pp.
- Mancktelow N (1985) The Simplon line: a major displacement zone in the western Lepontine Alps. Eclogae geol. Helv. 78, 73-96.
- Martinotti G Per Enel Produzione (1993) Impianto di Piedilago - Studio geologico strutturale e idrologico "*Piedilago Plant - Geological, structural and hydrologic study*". Rapporto finale del 30 aprile 1993.
- Martinotti G, Marini L, Hunziker J C, Perello P, Pastorelli S (1999) Geochemical and geothermal study of springs in the Ossola-Simplon Region, in Eclogae geol. Helv. 92 (1999), pp. 295-305.
- Masset O, Loew S (2010) Hydraulic conductivity distribution in crystalline rocks, derived from inflows to tunnels and galleries in the Central Alps, Switzerland. Hydrogeology Journal, 18, pp. 863-891.
- Maxelon M, Mancktelow N (2005) Three-dimensional geometry and tectonostratigraphy of the Pennine zone, Central Alps; Switzerland and Northern Italy. Earth-Science Reviews, 71, 171-227.
- McDonald MG, Harbaugh AW (1988) A Modular Three-Dimensional Finite-Difference Ground-Water Flow Model - U.S. Geological Survey, Techniques of Water-Resources Investigations, Book 6, Chapter A1
- Mehl SW, Hill MC (2001) MODFLOW-2000, The U.S. Geological Survey Modular Ground-Water Model - User Guide to the Link-Amg (LMG) Package for Solving Matrix Equations Using an Algebraic Multigrid Solver: U.S. Geological Survey Open-File Report 01-177, 33 p.
- Milnes AG, Grellier M, Müller R (1981) Sequence and style of major post-nappe structures, Simplon-Pennine Alps. Journal of Structural Geology, 3, 411-420.
- Mun Y, Uchirin CG (2004) Development and Application of a MODFLOW Preprocessor Using Percolation Theory for Fractured Media. Journal of the American Water Resources Association, 40(1), 229-239.
- Pastorelli S, Marini L, Hunziker J (2001) Chemistry, isotop values (δD , $\delta^{18}O$, $\delta^{34}SSO_4$) and temperatures of the water inflows in two Gotthard tunnels, Swiss Alps, in Applied Geochemistry 16 (2001), pp. 633-649.
- Prudic DE (1989) Documentation of a computer program to simulate stream-aquifer relations using a modular, finite-difference, ground-water flow model. U.S. Geological Survey, Open-File Report 88-729.
- Schmidt C, Preiswerk H (1905) Geologische Karte der Simplongruppe. Beiträge zur Geologischen Karte der Schweiz, [N.F.] 26, Spezialkarte No. 48.
- Steck A (2008) Tectonics of the Simplon massif and Lepontine gneiss dome: deformation structures due to collision between the underthrusting European plate and the Adriatic indenter. Swiss Journal of Geoscience, 101, 515-546.
- Thapa BB, Nolting RM, Teske MJ, Mcrae MT (2005) "Predicted and observed groundwater inflows into two rock tunnels" - RECT Proceedings, Chapter 50, p. 556-567.
- Thornthwaite CW, Mather JR (1957) Instructions and tables for computing potential evapotranspiration and the water balance. Drexel Institute of Technology, Publications in Climatology, Vol. X, 3, 185-311 p, Centerton, New Jersey (USA).
- Urey HC, Lowenstam HA, Epstein S, McKinney CR (1951) Measurement of paleotemperatures and temperatures of the Upper Cretaceous of England, Denmark and the Southern United States. Geological Society of America Bulletin, 62, pp. 399-416.
- Zaadnoordijk WJ (2009) Simulating Piecewise-Linear Surface Water and Ground Water Interactions with MODFLOW. Ground Water, 47(5), 723-726
- Zheng C & Bennevay GD (1995) Applied contaminant transport modelling - Van Nostrand Reinhold ITP
- Zwingmann H, Mancktelow N (2004) Timing of Alpine fault gauges. Earth and Planetary Science Letters, 223, 415-425.